SoftwareX 6 (2017) 155–160

Contents lists available at ScienceDirect

SoftwareX

journal homepage: www.elsevier.com/locate/softx

CompSim: Cross sectional modeling of geometrical complex and inhomogeneous slender structures

Turaj Ashuri[a,*,1], Jie Zhang[b,1]

[a] Arkansas Tech University, Russellville, AR 72801, USA
[b] University of Texas at Dallas, Richardson, TX 78080, USA

ARTICLE INFO

Article history:
Received 30 May 2016
Received in revised form 24 March 2017
Accepted 12 April 2017

Keywords:
Structural properties
Cross sectional modeling
Inhomogeneous structures
Geometrical complex structures

ABSTRACT

Many engineering disciplines require a fast and accurate estimate of structural properties in initial design phase for analysis and optimization studies. This paper presents an open-source computational code named CompSim to develop the structural properties of complex geometries with inhomogeneous materials. Weighted average technique is used to compute properties such as stiffness coefficients, area moment of inertia, and mass distribution. The accuracy of the code is evaluated for a multi-layer composite cross-section. As an illustrative example, the properties of the 20 MW common research wind turbine model are computed and presented. The code helps users to develop and optimize an initial structure in conceptual and preliminary design for further analysis in detailed design phase.

Code metadata

Current code version	V1.0
Permanent link to code/repository used of this code version	https://github.com/ElsevierSoftwareX/SOFTX_SOFTX-D-16-00046
Legal Code License	MATLAB Site-License (University of Texas at Dallas, License Number: 706581)
Code versioning system used	git
Software code languages, tools, and services used	Matlab R2013b
Compilation requirements, operating environments & dependencies	Windows, Linux, Mac
Link to developer documentation/manual	https://github.com/tashuri/compsim/
Support email for questions	turaj.ashuri@gmail.com

1. Introduction

In many engineering disciplines such as mechanical, civil, aerospace, and naval, the structure is subjected to external wind, seismic and wave loading, and needs to be designed accordingly [1–9]. These engineering structures require the definition of structural properties like stiffness coefficients, area moment of inertia, and mass distribution for aeroelastic and hydroelastic analysis,[2] and design [10–16]. Typically, finite element models are used to compute these properties as inputs for time or frequency domain analysis [17–22]. However, such finite element models are of value in investigating the local distribution of the strains and stresses within the structure, and therefore not suitable for the conceptual and preliminary design phase [23]. They are computationally expensive, and very detailed for global aeroelastic and hydroelastic design that in general only requires mass and stiffness distribution of the structure.

To overcome the complicated use of finite element models, many studies use simple geometric models of the cross-section

---

* Corresponding author.
E-mail address: turaj.ashuri@gmail.com (T. Ashuri).

[1] Assistant Professor

[2] Aeroelasticity and hydroelasticity are branches of physics to study the interactions among inertial, elastic, and aerodynamic or hydrodynamic forces for elastic bodies exposed to a fluid flow. Aeroelastic and hydroelastic effects are important design considerations for slender beam structures such as wind turbine and helicopter blades, aircraft wings, ship propellers, and tall buildings. Therefore, the designer needs to compute structural properties such as mass and stiffness distribution that have dependency on the inhomogeneous materials across a complex geometry.

http://dx.doi.org/10.1016/j.softx.2017.04.003
2352-7110/

such as I-Beams [24,25]. These simplified models can represent the mass and stiffness distribution of the structure, but model parameters need to be adjusted with measurements to guarantee their accuracy. Such a parameter tuning can increase the accuracy in a given point within the design space, but overall the accuracy cannot be guaranteed in the entire design space. This is a problem in optimization studies, since the optimizer searches the entire feasible range of a parameter for an optimal solution. Therefore, the accuracy of the model becomes questionable if the optimizer changes the model parameters beyond their adjusted point.

The computational code presented in this paper, named CompSim, provides a new methodology for extracting properties of complex geometrical structures with inhomogeneous materials for conceptual and preliminary design phase. It can also be used as a complementary tool for trade-off studies in detailed design stage by providing initial design candidates. CompSim uses a weighted average technique combined with Euler–Bernoulli beam theory to extract the structural properties [26,27]. This is explained in next section.

2. Software description

Typically, slender beam cross-sections consist of several structural elements such as shear-webs, spar-caps, and a shell as depicted in Fig. 1. The shear-webs provide shear capacity for the structure. The spar-caps increase the bending capacity, and the shell encloses the structure and provides torsional resistance. For such a beam, certain assumptions based on Euler–Bernoulli beam theory are made to extract the structural properties of the cross-section [26,27]. These are:

- The strain is proportional to the distance from the neutral axis;
- Beam transverse deflections remain small; and
- Plane sections of the beam remain plane and perpendicular to the neutral axis.

Fig. 1 shows a lifting-surface cross-section that has different material properties. A weighting method is used to extract the equivalent properties of this cross-section. This allows one to represent the complex inhomogeneous distribution of materials with a gross representation and equivalent properties [28]. The actual thickness of each cross sectional element is maintained to be used for extracting weights.

As depicted in Fig. 2, the equivalent modulus of elasticity of the shell, $E_{equivalent}^{shell}$, made of some ±45° composite lamina on top, t_{top}^{shell}, and bottom, t_{bottom}^{shell}, and a foam in between with a modulus of elasticity of E_{foam}^{shell} and thickness of t_{foam}^{shell} can be computed as:

$$E_{equivalent}^{shell} = \frac{\sum_{1}^{n} E_i^{shell}\ t_i^{shell}}{\sum_{1}^{n} t_{equivalent}^{shell}} \tag{1}$$

where the index i represents different materials used in the shell:

$$\sum_{1}^{n} E_i^{shell}\ t_i^{shell} = E_{top}^{shell}\ t_{top}^{shell} + E_{bottom}^{shell}\ t_{bottom}^{shell} + E_{foam}^{shell}\ t_{foam}^{shell}. \tag{2}$$

In this formulation, the total thickness of the shell remains the same:

$$\sum_{1}^{n} t_{equivalent}^{shell} = t_{top}^{shell} + t_{bottom}^{shell} + t_{foam}^{shell}. \tag{3}$$

The same approach is used to extract the equivalent densities of each element of the cross-section. In this case, the modulus of elasticity has to be replaced with the density.

Section centroid in flapwise direction, $\bar{X}_c^{section}$, is computed as:

$$\bar{X}_c^{section} = \frac{\sum_{1}^{m} E_{equivalent}^{j}\ A_{equivalent}^{j}\ \bar{X}_c^{j}}{\sum_{1}^{m} E_{equivalent}^{j}\ A_{equivalent}^{j}} \tag{4}$$

where the index j represents different structural elements of the cross-section, A is the cross-sectional area of the structural element, and denominator and numerator are defined as:

$$\begin{aligned}\sum_{1}^{m} E_{equivalent}^{j}\ A_{equivalent}^{j}\ \bar{X}_c^{j} = {} & E_{equivalent}^{shell}\ A_{equivalent}^{shell}\ \bar{X}_c^{shell}\\ & + E_{equivalent}^{spar}\ A_{equivalent}^{spar}\ \bar{X}_c^{spar}\\ & + E_{equivalent}^{web}\ A_{equivalent}^{web}\ \bar{X}_c^{web}\end{aligned} \tag{5}$$

and:

$$\begin{aligned}\sum_{1}^{m} E_{equivalent}^{j}\ A_{equivalent}^{j} = {} & E_{equivalent}^{shell}\ A_{equivalent}^{shell}\\ & + E_{equivalent}^{spar}\ A_{equivalent}^{spar}\\ & + E_{equivalent}^{web}\ A_{equivalent}^{web}.\end{aligned} \tag{6}$$

Similarly, for the section centroid in edgewise direction, $\bar{Y}_c^{section}$, we have:

$$\bar{Y}_c^{section} = \frac{\sum_{1}^{m} E_{equivalent}^{j}\ A_{equivalent}^{j}\ \bar{Y}_c^{j}}{\sum_{1}^{m} E_{equivalent}^{j}\ A_{equivalent}^{j}}. \tag{7}$$

In this equation, the denominator is the same as Eq. (6), but the numerator is defined as:

$$\begin{aligned}\sum_{1}^{m} E_{equivalent}^{j}\ A_{equivalent}^{j}\ \bar{Y}_c^{j} = {} & E_{equivalent}^{shell}\ A_{equivalent}^{shell}\ \bar{Y}_c^{shell}\\ & + E_{equivalent}^{spar}\ A_{equivalent}^{spar}\ \bar{Y}_c^{spar}\\ & + E_{equivalent}^{web}\ A_{equivalent}^{web}\ \bar{Y}_c^{web}.\end{aligned} \tag{8}$$

These section centroids are used to transfer the area moments of inertia using parallel-axis theorem to any axis of interest [29]. Area moments of inertia are calculated by an integration scheme [30]. Here, the cross-section $x-y$ coordinates of spar-caps, shell and shear-webs are used separately to compute the area moment of inertia with respect to their local axis. As an example, the integrals for the shell are as follows:

$$I_{xx}^{shell} = \int y_{shell}^2\, dx\, dy \tag{9}$$

$$I_{yy}^{shell} = \int x_{shell}^2\, dx\, dy \tag{10}$$

$$I_{xy}^{shell} = \int x_{shell}\, y_{shell}\, dx\, dy. \tag{11}$$

These calculated area moments of inertia need to be transferred to the section centroids using the parallel-axis theorem. This is given for the shell by:

$$I_{xx}^{SHELL} = I_{xx}^{shell} + A_{shell}\left(\bar{X}_c^{shell} - \bar{X}_c^{section}\right)^2 \tag{12}$$

$$I_{yy}^{SHELL} = I_{yy}^{shell} + A_{shell}\left(\bar{Y}_c^{shell} - \bar{Y}_c^{section}\right)^2 \tag{13}$$

$$I_{xy}^{SHELL} = I_{xy}^{shell} + A_{shell}\left(\bar{X}_c^{shell} - \bar{X}_c^{section}\right)\left(\bar{Y}_c^{shell} - \bar{Y}_c^{section}\right). \tag{14}$$

Note that small *shell* refers to local centroids, and capital *SHELL* refers to section centroids. These area moments of inertia can also

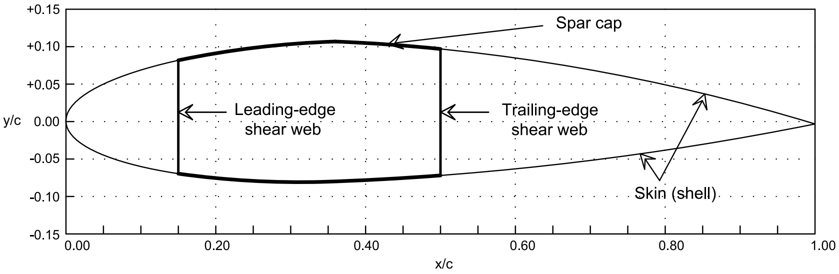

Fig. 1. Cross-section of a typical lifting surface device consisting of several different structural elements. y/c and x/c are the normalized thickness and chord of the cross section, respectively.

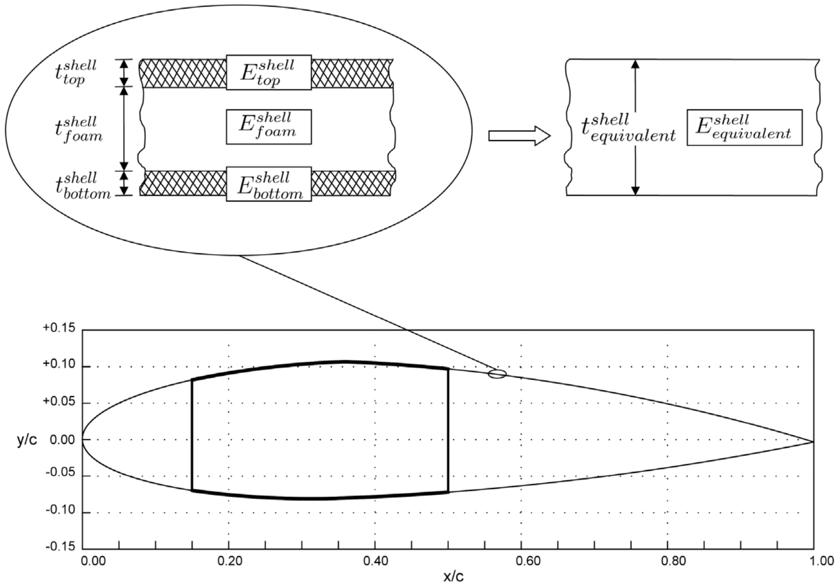

Fig. 2. Equivalent representation of properties. The figure presents different materials that are used to construct the shell. These different materials are lumped together to have an equivalent material with the same properties as the multi-layer shell.

be rotated at any rotation angle, θ, around any arbitrary axis using a tensor transformation [31] as:

$$I^{SHELL}_{x'x'} = \frac{I^{SHELL}_{xx} + I^{SHELL}_{yy}}{2} + \frac{I^{SHELL}_{xx} - I^{SHELL}_{yy}}{2} \cos 2\theta - I^{SHELL}_{xy} \sin 2\theta \quad (15)$$

$$I^{SHELL}_{y'y'} = \frac{I^{SHELL}_{xx} + I^{SHELL}_{yy}}{2} + \frac{I^{SHELL}_{xx} - I^{SHELL}_{yy}}{2} \cos 2\theta + I^{SHELL}_{xy} \sin 2\theta \quad (16)$$

$$I^{SHELL}_{x'y'} = \frac{I^{SHELL}_{xx} - I^{SHELL}_{yy}}{2} \sin 2\theta + I^{SHELL}_{xy} \cos 2\theta \quad (17)$$

Using the calculated flapwise area moment of inertia and equivalent modulus of elasticity, section flapwise stiffness can be calculated as:

$$\begin{aligned} E^{sec\,tion}_{total}\, I^{sec\,tion}_{xx} &= E^{shell}_{equivalent}\, I^{SHELL}_{xx} \\ &\quad + E^{spar}_{equivalent}\, I^{SPAR}_{xx} \\ &\quad + E^{web}_{equivalent}\, I^{WEB}_{xx}. \end{aligned} \quad (18)$$

The same formulation can be used to compute the edgewise stiffness. Mass distribution for an arbitrary cross-section with length L is computed as:

$$\begin{aligned} \left(\frac{M}{L}\right)_{station} &= \rho^{shell}_{equivalent}\, A^{shell}_{equivallent} \\ &\quad + \rho^{spar}_{equivalent}\, A^{spar}_{equivallent} \\ &\quad + \rho^{web}_{equivalent}\, A^{web}_{equivallent} \end{aligned} \quad (19)$$

where ρ is the density, and L is the length of each spatially discretized section.

Knowing the mass distribution, the total mass of k spatially discretized stations can be defined as:

$$M_{blade} = \sum_{1}^{k} \left(\frac{M}{L}\right)_{k} L_{k}. \quad (20)$$

The source code for modeling the cross sectional properties is written in MATLAB. The main parts of the source code are the definition of the input data, computation of the properties, and outputs as explained next.

2.1. Input data

To compute the properties of any arbitrary structure, two different categories of input data are required. First, the geometry of the structure has to be defined. Second, the materials that are used to construct the geometry have to be provided. Next subsection explains how to define these properties as an input by the user.

2.1.1. Geometrical properties

The geometry can be defined in terms of $x-y$ coordinates in non-dimension form. These coordinates have to be put into separate files, and defined for different cross-sections of the structure. The user has the choice to make any geometry of interest as long as the choice of $x-y$ coordinates is consistent and results into a closed geometry. For example, the geometry of the *NACA64-618* can be defined as [32]:

```
% An example of how the format of an airfoil input data should look like
NACA64—618 airfoil x—y coordinates file
      1.000000      0.000000
      0.995801      0.001118
      0.989133      0.002901
        ...            ...
```

The first column in this file is the x coordinate of the airfoil, and the second column is the y coordinate. Upon connecting these $x-y$ coordinates the external shape of the cross-section is obtained. These coordinate files, 'AirFolCordName', have to be put in the right order from the root of the structure to its tip at some discrete sections for constructing the entire geometry. The location of each cross-section can be controlled in a non-dimension form using 'BeamFract' array. The user can twist these cross-sections at any angle of interest along the normalized chord, 'PichAxis'.

```
% Array with the name of all the x-y coordinate input files for each cross-
      section
AirFolCordName = ['Cylinder1.dat'; ... ; 'NACA64618.dat'];

% Location of each cross-section where the inputs are defined and the
      properties computed.
BeamFract = [0.0000 ... 1.0000];

% Non-dimension chordwise location for structural twist measured from leading
      -edge for each x-y airfoil file
PichAxis = [0.5 ... 0.175];
```

2.1.2. *Material and structural properties*

Material and structural properties are the modulus of elasticity, shear modulus, density and the thickness for shell, spar-caps and shear-webs, as well as the total length of the structure. While a structural element has fixed material properties at all different cross-sections, it can have variable structural thicknesses defined from the root to the tip. The user needs to make a consistent choice of units, and no units are specifically assigned to a property by the code.

```
% Length of the slender beam structure
BeamLngth = 135;

% Structural twist of each cross-section defined rotated around the
      $PichAxis$
StrcTwst = [14.7607; ... ; 0.0000];

% Structural chord
StrcChrd = [3.5420; ... ; 1.7160];

% Thickness of the spar-cap along the structure
SparTick = [0.1500; ... ; 0.1000];

% Thickness of the shear-webs along the structure
WebTick = [0.2000; ... ; 0.1000];

% Thickness of the shell along the structure
ShllTick = [0.2500; ... ; 0.1500];

% Location of the first and second shear-web along the chord measured from
      the leading-edge
Web1LocProf=0.15;
Web2LocProf=0.50

% Modulus of elasticity of the shell in Ex (chordwise) and Ey (flapwise)
      direction
ShllModulElstX=17E9;
ShllModulElstY=17E9;

% Modulus of the elasticity of the spar-cap in Ex (chordwise) and Ey (
      flapwise) direction
SparModulElstX=32E9;
SparModulElstY=32E9;

% Modulus of the elasticity of the shear-web in Ex (chordwise) and Ey (
      flapwise) direction
WebModulElstX=17E9;
WebModulElstY=17E9;

% Density of the Shell
ShllRho=510;

% Density of the shear-web
WebRho=510;

% Density of the Spar-cap
SparRho=690;
```

2.2. *Computation of the structural properties*

A chain of computations is performed to find the structural properties of the slender beam structure, taking into account the complex geometry and different material properties. As an outcome, the code computes properties such as mass, flapwise, edgewise, and mass distribution along the structure.

Table 1
Comparison of stiffness coefficients of the multi-layered composite structure.

Code	EI_{22}	EI_{33}	GJ	EA
VABS	5.40E+03	1.55E+04	1.97E+03	4.62E+07
CompSim	7.11E+03	2.09E+04	3.20E+03	5.83E+07
Rel. diff. (%)	31.7	34.8	62.4	26.1

2.3. *Output file*

Once all the properties are computed, they are written to a text file. In addition to the standard properties explained above, several other useful detailed properties such as the area moment of inertia of each cross-section, the mass moment of inertia, and shear and torsional stiffness are computed. The code also plots automatically the mass distribution, flapwise and edgewise stiffness distribution, as well as the external geometry of the structure as presented in Section 4.

3. Verification and validation

To assess and evaluate the accuracy of the code, a multi-layer composite cross-section with the geometry and the lamination data presented in Fig. 3 is used. This is a thin-walled cross-section that has a wall thickness to chord ratio of less than 0.1 [33]. The composite material properties are $E_{11} = 142.0$ GPa, $E_{22} = E_{33} = 9.8$ GPa, and $G_{12} = G_{13} = G_{23} = 60.0$ GPa.

A comparison is made with VABS that is a cross sectional analysis code for modeling initially curved and pre-twisted anisotropic structures for arbitrary topology and material distributions [35]. Table 1 shows the sectional stiffness coefficients for the presented cross-section of Fig. 3.

As the table shows, considerable differences exist between CompSim and VABS predictions. In general, little agreement exists among different computational codes to model the structural properties, and up to 337% relative difference is reported in the literature [34]. This is due to different assumptions and simplifications used to model the structure.

The loss of accuracy in CompSim is related to the smeared approach to simplify the problem. In smeared approach, the cross-section is modeled as a single layer with the material properties being assumed as the average of the properties of all the layers. While such an approach is suitable for fast analysis in conceptual and preliminary design phase, it lacks accuracy for detailed design as presented in this section. Therefore, for detailed design analysis, the use of finite element based computational codes such as VABS, FAROB, BECAS and CROSTAB is recommended [36–39].

4. Illustrative examples

We used the developed method and code in several of our recent studies [40–44]. As an illustrative example, modeling the structural properties of a 20 MW wind turbine blade is considered in this paper. The input data of the blade can be found in [45].

The blade internal architecture consists of a shell, two spar-caps and two shear-webs similar to Fig. 1. The blade external shape has a circular cross-section at the blade root and 6 airfoil types from the root to the tip. The $x-y$ coordinates of the blade are defined at 20 different discrete sections of the blade, along with their corresponding chord and twist distribution. Fig. 4a shows the cross sectional details of the blade, and Fig. 4b depicts the external shape of the 20 MW blade.

Based on these inputs, structural properties of the blade are computed. Fig. 5 shows the mass distribution of the blade along the span. Using this mass distribution, the total estimated mass of the blade is 259567 kg. The blade flapwise and edgewise stiffness are shown in Fig. 6.

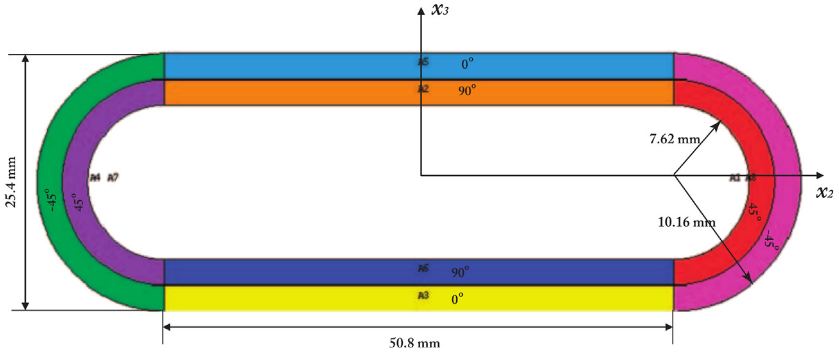

Fig. 3. Cross-section of the multi-layer composite structure [34]. The cross-section has 0° and 90° fibers to represent the spar, and ± 45° fibers to represent the shell.

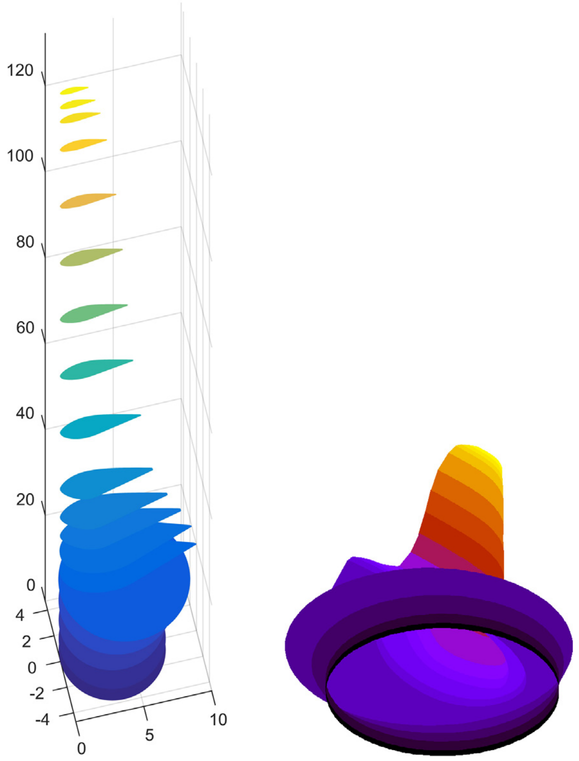

(a) Cross sectional details.

(b) External shape.

Fig. 4. The geometry of the common 20 MW research wind turbine model. For this model, the $x-y$ coordinates are used to define the cross-sectional details (a). These cross-sections are then used to make the external geometry of the blade (b).

5. Impact

This publicly available free source code is capable of modeling cross sectional properties of complex beam structures in several different fields of engineering [46–52]. It helps the users to save time by providing a simple tool for conceptual and preliminary design, instead of using complex and time consuming finite element codes. It also allows users optimizing such an initial design when coupled with an optimizer. Therefore, it is expected that researchers and engineers across several engineering disciplines to use the code.

6. Conclusions

In any structural design study that involves complex geometry and materials of different types, structural properties such as area and mass moment of inertia, stiffness, and mass per unit length are needed. These properties are used to compute natural frequencies, deflections, buckling, stresses, fatigue damage and so on. CompSim extracts these properties for any arbitrary cross-section of a structure made of multiple materials, and it is suitable for fast analysis in conceptual and preliminary design phase. However, in detailed and final design studies, the use of finite element computational codes is recommended.

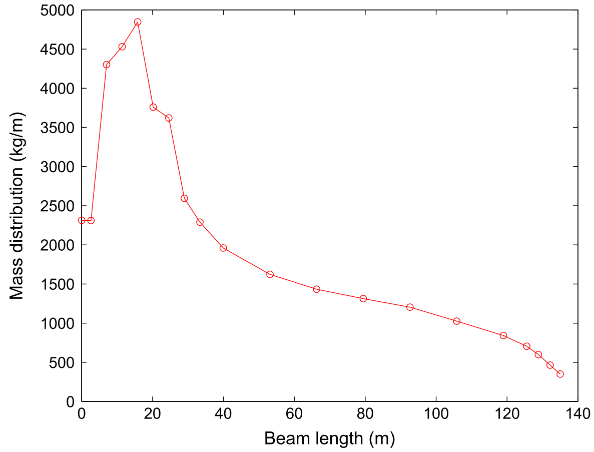

Fig. 5. Mass distribution of the 20 MW common research wind turbine model along the blade length.

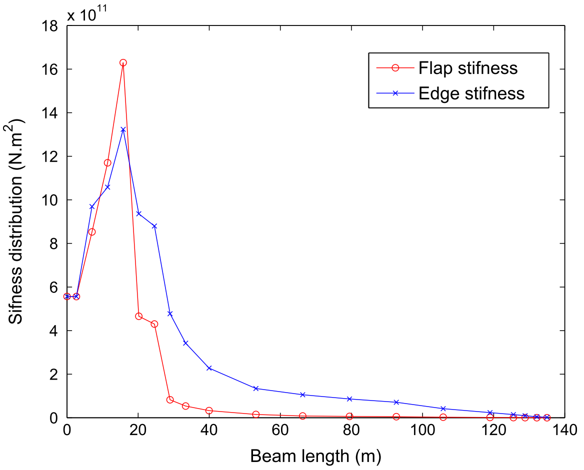

Fig. 6. Flapwise and edgewise stiffness distribution of the 20 MW common research wind turbine model along the blade length.

Acknowledgment

This research was part of the UpWind project supported by the European Union sixth framework program, grant number 019945 (2006–2011). The financial support is greatly acknowledged.

References

[1] Simiu Emil, Scanlan Robert H. Wind effects on structures. Wiley; 1996.

[2] Lam Dennis, Gardner Leroy. Structural design of stainless steel concrete filled columns. J Construct Steel Res 2008;64(11):1275–82.

[3] Hansen Lars U, Horst Peter. Multilevel optimization in aircraft structural design evaluation. Comput Struct 2008;86(1):104–18.

[4] Vanem Erik, Bitner-Gregersen Elzbieta M. Stochastic modelling of long-term trends in the wave climate and its potential impact on ship structural loads. Appl Ocean Res 2012;37:235–48.

[5] Perea Cristian, Alcala Julian, Yepes Victor, Gonzalez-Vidosa Fernando, Hospitaler Antonio. Design of reinforced concrete bridge frames by heuristic optimization. Adv Eng Softw 2008;39(8):676–88.

[6] Espinosa Horacio Dante, Lee S, Moldovan N. A novel fluid structure interaction experiment to investigate deformation of structural elements subjected to impulsive loading. Exp Mech 2006;46(6):805–24.

[7] Mylonakis George, Nikolaou Sissy, Gazetas George. Footings under seismic loading: Analysis and design issues with emphasis on bridge foundations. Soil Dyn Earthq Eng 2006;26(9):824–53.

[8] Luo M, Zhu WQ. Nonlinear stochastic optimal control of offshore platforms under wave loading. J Sound Vib 2006;296(4):734–45.

[9] Leishman J Gordon. Challenges in modeling the unsteady aerodynamics of wind turbines. In: ASME 2002 Wind Energy Symposium. American Society of Mechanical Engineers; 2002. p. 141–67.

[10] Dowell Earl, Edwards John, Strganac Thomas. Nonlinear aeroelasticity. J Aircr 2003;40(5):857–74.

[11] Chen Xu-jun, Wu You-sheng, Cui Wei-cheng, Jensen J Juncher. Review of hydroelasticity theories for global response of marine structures. Ocean Eng 2006;33(3):439–57.

[12] Ashuri Turaj. Beyond classical upscaling: integrated aeroservoelastic design and optimization of large offshore wind turbines, PhD Thesis. Delft University of Technology, the Netherlands; 2012.

[13] Murugan Senthil, Ganguli Ranjan, Harursampath Dineshkumar. Aeroelastic response of composite helicopter rotor with random material properties. J Aircr 2008;45(1):306–22.

[14] Su Weihua, Cesnik Carlos ES. Nonlinear aeroelasticity of a very flexible blended-wing-body aircraft. J Aircr 2010;47(5):1539–53.

[15] Mulcahy NL, Prusty BG, Gardiner CP. Hydroelastic tailoring of flexible composite propellers. Ships Offshore Struct 2010;5(4):359–70.

[16] Braun Alexandre Luis, Awruch Armando Miguel. Aerodynamic and aeroelastic analyses on the CAARC standard tall building model using numerical simulation. Comput Struct 2009;87(9):564–81.

[17] Bauchau Olivier A, Bottasso Carlo L, Nikishkov Yuri G. Modeling rotorcraft dynamics with finite element multibody procedures. Math Comput Modelling 2001;33(10):1113–37.

[18] Wang Qi, Yu Wenbin. Variational-asymptotic modeling of the thermoelastic behavior of composite beams. Compos Struct 2011;93(9):2330–9.

[19] Blasques JP, Bitsche RD, Fedorov V, Lazarov BS. Accuracy of an efficient framework for structural analysis of wind turbine blades. Wind Energy 2015;19(9):1603–21.

[20] Blasques JP, Lazarov B. BECAS V2, A cross-section analysis tool for anisotropic and inhomogeneous beam sections of arbitrary geometry. 2012.

[21] Wang Qi, Johnson Nick, Sprague Michael A, Jonkman Jason. BeamDyn: A High-Fidelity Wind Turbine Blade Solver in the FAST Modular Framework. In: 33rd Wind energy symposium, American Institute of Aeronautics and Astronautics. 2015. p. 1–17.

[22] Ashuri Turaj, van Bussel Gerard JW, Mieras Stefan. Development and validation of a computational model for design analysis of a novel marine turbine. Wind Energy 2013;16(1):77–90.

[23] Malcolm David J, Laird Daniel L. Extraction of equivalent beam properties from blade models. Wind Energy 2007;10(2):135–57.

[24] Fuglsang P, Madsen H Aagaard. Optimization method for wind turbine rotors. J Wind Eng Ind Aerodyn 1999;80(1):191–206.

[25] Benini Ernesto, Toffolo Andrea. Optimal design of horizontal-axis wind turbines using blade-element theory and evolutionary computation. J Sol Energy Eng 2002;124(4):357–63.

[26] Biondi B, Caddemi S. Closed form solutions of Euler–Bernoulli beams with singularities. Int J Solids Struct 2005;42(9):3027–44.

[27] Bauchau OA, Craig JI. Euler-Bernoulli beam theory. In: Structural analysis. Springer; 2009. p. 173–221.

[28] Ashuri Turaj, Van Bussel Gerard JW, Zaayer Michiel B, Van Kuik Gijs AM. An analytical model to extract wind turbine blade structural properties for optimization and up-scaling studies. In: The science of making torque from wind, Heraklion, Crete, Greece. European Wind Energy Association; 2010. p. 1–7.

[29] Jones Robert M. Mechanics of composite materials. Scripta Book Company Washington, DC; 1975.

[30] Davis Philip J, Rabinowitz Philip. Methods of numerical integration. Courier Corporation; 2007.

[31] Ashuri Turaj. Introduction to continuum mechanics: theory and practise. Arkansas Tech University; 2016.

[32] Eppler Richard. Airfoil design and data. Springer Science & Business Media; 1990.

[33] Bischoff M, Bletzinger K-U, Wall WA, Ramm E. Models and finite elements for thin-walled structures. Encyclopedia of computational mechanics, Wiley Online Library; 2004.

[34] Chen Hui, Yu Wenbin, Capellaro Mark. A critical assessment of computer tools for calculating composite wind turbine blade properties. Wind Energy 2010;13(6):497–516.

[35] Yu Wenbin, Hodges Dewey H, Volovoi Vitali, Cesnik Carlos ES. On Timoshenko-like modeling of initially curved and twisted composite beams. Int J Solids Struct 2002;39(19):5101–21.

[36] Cesnik Carlos ES, Hodges Dewey H. VABS: a new concept for composite rotor blade cross-sectional modeling. J Am Helicopter Soc 1997;42(1):27–38.

[37] Lindenburg Corton, Hegberg T. PHATAS–IV, User's manual. 1999.

[38] Blasques José Pedro Albergaria Amaral, Bitsche Robert, Fedorov Vladimir, Eder Martin Alexander. Applications of the beam cross section analysis software (BECAS). In: 26th nordic seminar on computational mechanics. 2013. p. 46–9.

[39] Lindenburg Corton, STABLAD, Stability analysis Tools for Anisotropic rotor BLADe panels, 590, 1999.

[40] Ashuri Turaj, Zaaijer Michiel B, Martins Joaquim RRA, van Bussel Gerard JW, van Kuik Gijs AM. Multidisciplinary design optimization of offshore wind turbines for minimum levelized cost of energy. Renew Energy 2014;68(0):893–905.

[41] Ashuri Turaj, Rotea Mario, Xiao Yan, Li Yaoyu, Ponnurangam Chandra Verma. Wind turbine performance decline and its mitigation via extremum seeking controls. In: AIAA science and technology forum and exposition (SciTech), Wind Energy Symposium, San Diego, California. American Institute of Aeronautics and Astronautics; 2016. p. 1–11.

[42] Ashuri Turaj, Zhang Tao, Qian Dong, Rotea Mario. Uncertainty quantification of the levelized cost of energy for the 20MW research wind turbine model. In: AIAA science and technology forum and exposition (SciTech), Wind Energy Symposium, San Diego, California. American Institute of Aeronautics and Astronautics; 2016. p. 1998.

[43] Ashuri Turaj, Zaaijer Michiel B, Martins Joaquim RRA, Zhang Jie. Multidisciplinary design optimization of large wind turbines–Technical, economic, and design challenges. Energy Convers Manage 2016;123:56–70.

[44] Ashuri Turaj, Van Bussel Gerard JW, Zaaijer Michiel B, Van Kuik Gijs AM. Controller design automation for aeroservoelastic design optimization of wind turbines. In: The science of making torque from wind, Heraklion, Crete, Greece. European Wind Energy Association; 2010. p. 1–7.

[45] Ashuri Turaj, Martins Joaquim RRA, Zaaijer Michiel B, van Kuik Gijs AM, van Bussel Gerard JW. Aeroservoelastic design definition of a 20 MW common research wind turbine model. Wind Energy 2016;19(11):2071–87.

[46] Sessarego Matias, Dixon KR, Rival DE, Wood DH. A hybrid multi-objective evolutionary algorithm for wind-turbine blade optimization. Eng Optim 2015;47(8):1043–62.

[47] Haghi Rad, Ashuri Turaj, van der Valk Paul LC, Molenaar David P. Integrated multidisciplinary constrained optimization of offshore support structures. J Phys Conf Ser 2014;555(1):012046.

[48] Caboni Marco. Probabilistic design optimization of horizontal axis wind turbine rotors. University of Glasgow, UK; 2016.

[49] Van Der Meulen Michiel B, Ashuri Turaj, Van Bussel Gerard JW, Molenaar David P. Influence of nonlinear irregular waves on the fatigue loads of an offshore wind turbine. In: The science of making torque from wind, Oldenburg, Germany. Citeseer; 2012. p. 1–10.

[50] Capponi Pablo Castillo, Ashuri Turaj, van Bussel Gerard JW, Kallesøe Bjarne. A non-linear upscaling approach for wind turbine blades based on stresses. In: European wind energy conference and exhibition, Brussels, Belgium. The European wind energy association; 2011. p. 1–8.

[51] Ashuri Turaj, Ponnurangam Chandra, Zhang Jie, Rotea Mario. Integrated layout and support structure optimization for offshore wind farm design. J Phys Conf Ser 2016;753(9):092011.

[52] van den Broek Sander F. Towards high-fidelity aeroelastic analysis of wind turbines, MSc Thesis. Delft University of Technology, the Netherlands; 2013.